

<https://doi.org/10.3176/oil.1999.2.04>

CHARACTERISTICS OF NO_x EMISSION IN FLUIDIZED BED COMBUSTION OF OIL SHALE

LI SHUYUAN, WANG GUOJIN
WANG JIANQIU, QIAN JIALIN

*School of Chemical Engineering
University of Petroleum
Changping 102200
Beijing, China*

In this paper, the combustion experiments on oil shale particles (3-5 mm in diameter) were carried out using a bench scale fluidized bed reactor. The characteristics of NO_x emission and the effects of several factors in oil shale combustion were investigated. The results indicated that bed temperature, particle diameter and moisture of oil shale have important influences on NO_x emission, and while limestone or shale ash added to the bed for SO_x capture has no effects. On the basis of data concerning NO_x concentration vs. time, an unreacted core model was developed. The model predictions agree reasonably well with experimental data.

Introduction

Oil shale is a kind of lean solid fossil fuels consisting mainly of mineral (~80 %) and organic matter (~20 %). Its resources are abundant throughout the world. As a kind of low calorific value fuel, oil shale can be used for electrical power generation. In Estonia, there are two large electrical power stations with capacity of 1,800 MW each, where the oil shale boilers have been operating for several decades. In China, a small-scale oil shale power station with a capacity of 200,000 kW is being built in Maoming Petrochemical Corporation, which will burn about 4 million tons of oil shale each year. This station was planned to be finished by the year 1996, and to be put into operation in 1997 to provide electrical power for Maoming Ethylene Factory. The key equipment of the power plant, circulating fluidized bed and the complete set of boiler installations will be imported from Ahlström Corporation.

At present, much attention has been paid to the environmental protection in the world. One of the most important problems to be solved in the development of coal combustion units is the abatement of SO_x and NO_x emissions. In recent years, a lot of basic investigations have been carried out on the release and capture of SO_x and NO_x during fluidized bed coal combustion around the world [1-3]. However, few of them were

concerned with the fluidized bed combustion of oil shale. Previous paper [4] reported a comprehensive model for the release and abatement of SO_x in fluidized bed combustion of oil shale. In this work, the characteristics of NO_x emission in fluidized bed oil shale combustion were investigated experimentally and theoretically. The effect of several factors (bed temperature, oil shale particle diameter, moisture content of oil shale, etc.) on NO_x emission was discussed on the basis of experimental data. The results obtained from this study will provide important information for controlling NO_x emission during the fluidized bed combustion of oil shale.

Experimental

In this work, oil shale sample was taken from Maoming, south of China. Its properties are as follows (wt%):

Moisture	6.97	C	17.47
Volatile	18.16	H	2.83
Ash	72.70	N	0.69
Fixed carbon	2.17	S	1.05
Calorific value (kJ/kg)	4200		

The batch analysis technique was used in this study. A batch bench-scale fluidized bed reactor with 63 mm diameter, 310 mm height was electrically heated, stainless steel vessel. Fluidizing gas, air, was supplied to the bed via the preheater and flowmeter. The other fittings, such as, internal distributor, external cyclone separator, oil shale inlet, shale ash outlet, etc., formed a complete system, similar to that used by Wang et al. [4]. A flue gas analyzer, with the model KNOS-600 (made in Japan), was connected to the vent of the reactor for monitoring NO_x concentration on line. The main experimental conditions are as follows:

Sample:	Maoming oil shale
Particle diameter:	0.5-5 mm
Ca/S molar ratio:	0-4.5
Air feeder:	7.0 m ³ /h
Bed temperature:	750-900 °C
Moisture content (wt%):	0-12 %
Shale ash added to the bed:	0-40 %
Sample feeder:	5.0 gm

Some of conditions above, such as, particle diameter, Ca/S molar ratio, bed temperature, moisture, are basically closed to those selected in Maoming power plant with a capacity of 35 ton/day. This plant has been operating for more than ten years. Ca/S molar ratio shows relative proportion of limestone to sulfur content in oil shale. And purpose of limestone, or shale ash, added into the bed is to capture SO_x from flue gas.

The typical experimental data are shown in Figures 1 and 2.

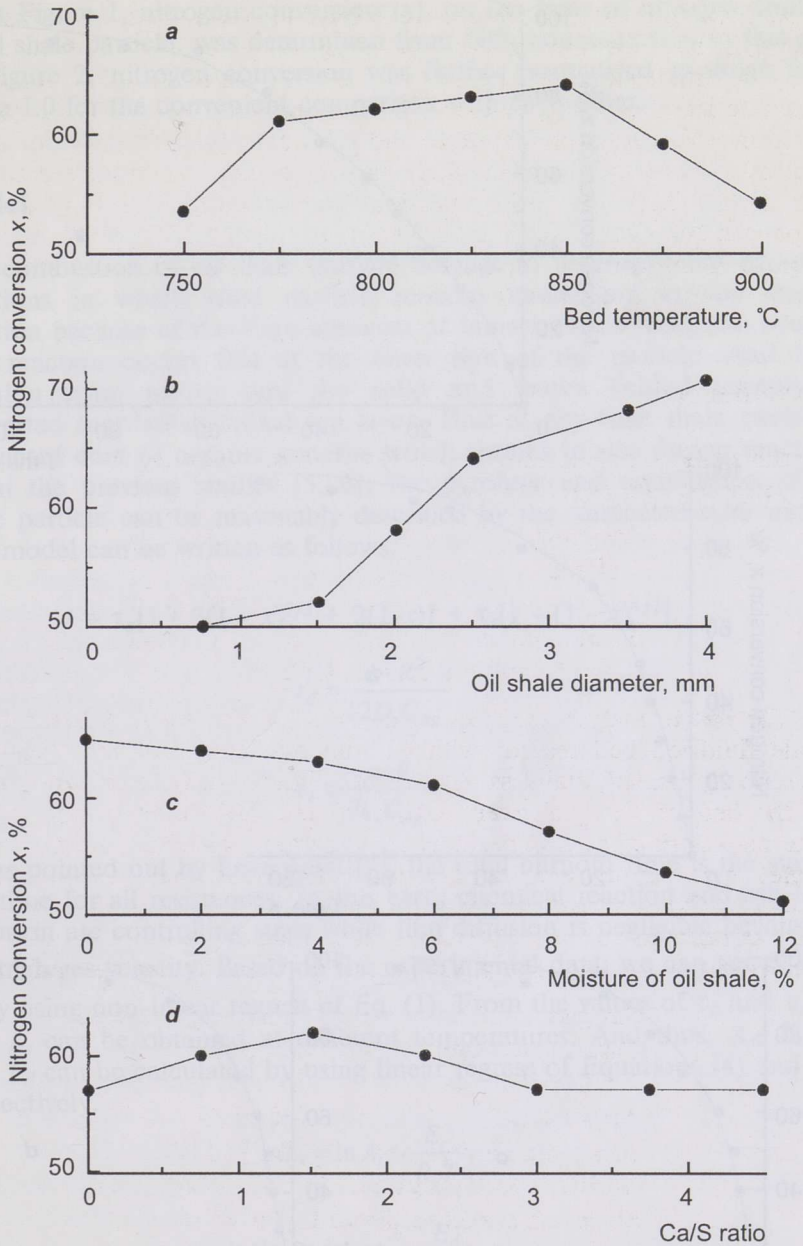


Fig. 1. The effect of (a) bed temperature, (b) particle diameter, (c) oil shale moisture, and (d) Ca/S molar ratio on NO_x emission

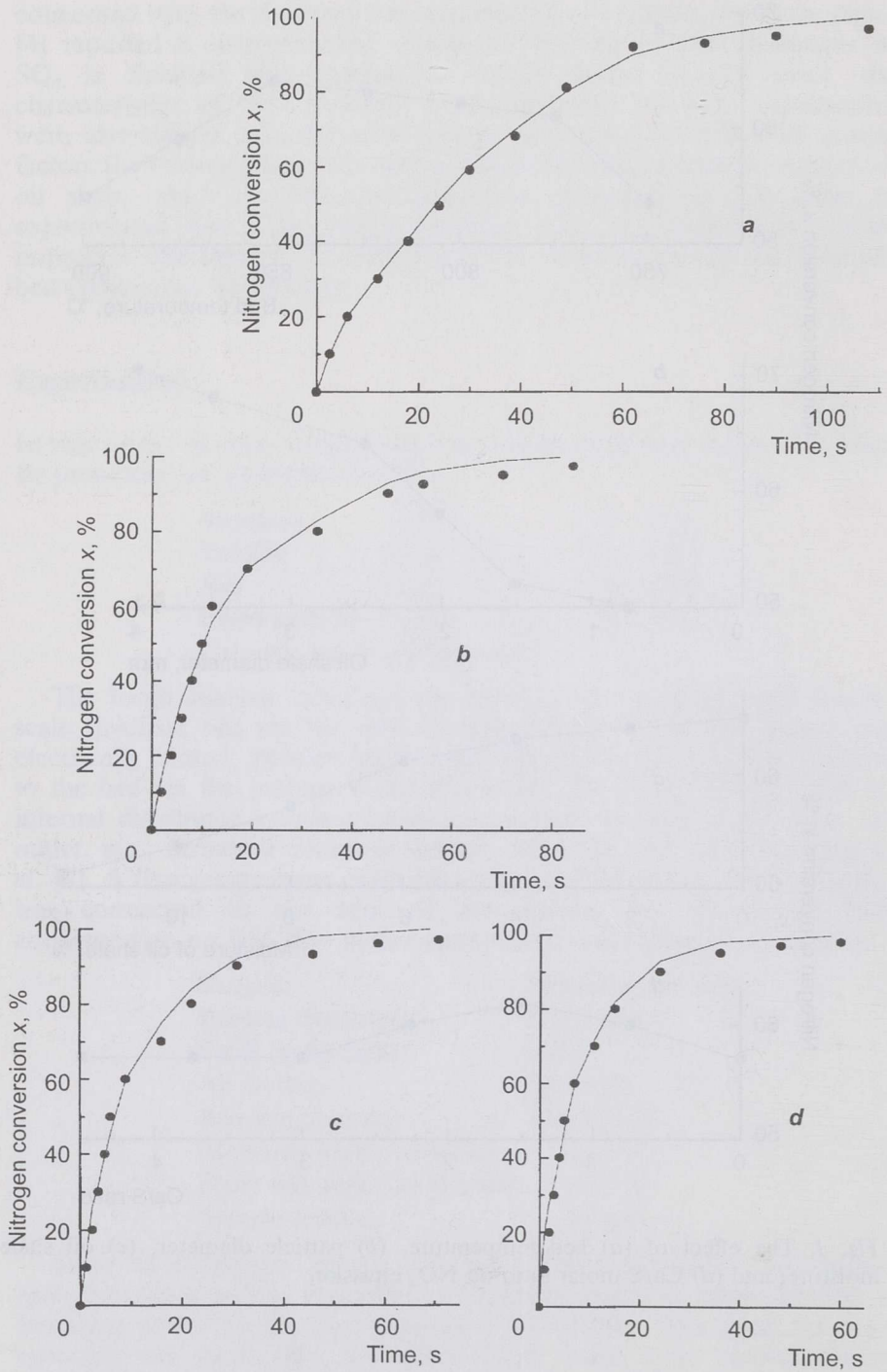


Fig. 2. Fractional conversion of nitrogen versus time (bed temperature (a) 750, (b) 800, (c) 850, and (d) 900; particle diameter 4 mm): curve — theory, points — experimental data

In Figure 1, nitrogen conversion (x), on the basis of nitrogen content in oil shale particle, was determined from NO_x concentration in flue gas. In Figure 2, nitrogen conversion was further normalized to range from 0.0 to 1.0 for the convenient comparison with each other.

Model

The combustion of oil shale particle belongs to heterogeneous gas-solid reactions in which solid particle remains unchanged in size during reaction because of the large amounts of impurities, or inorganic matter. The reaction occurs first at the outer skin of the particle. And then reaction zone moves into the solid and leaves behind completely converted inert solid, called ash layer. Thus at any time there exists an unreacted core of organic material which shrinks in size during reaction. From the previous studies [5, 6], the pyrolysis and combustion of oil shale particle can be reasonably described by the unreacted core model. The model can be written as follows:

$$t = \tau_a [1 - 3(1-x)^{2/3} + 2(1-x)] + \tau_r [1 - (1-x)^{1/3}] \quad (1)$$

$$\tau_a = \frac{\rho \cdot R^2}{12D_e C_{Ag}} \quad (2)$$

$$\tau_r = \frac{\rho \cdot R}{2k_s C_{Ag}} \quad (3)$$

As pointed out by Levenspiel [7], the total burnout time is the sum of the time for all resistances. In this case, chemical reaction and ash layer diffusion are controlling steps while film diffusion is negligible because of the high gas velocity. Based on the experimental data, we can get τ_a and τ_r by using non-linear regress of Eq. (1). From the values of τ_a and τ_r , D_e and k_s can be obtained at different temperatures. And thus, A_r , E_r , A_d and E_d can be calculated by using linear regress of Equations (4) and (5), respectively.

$$\ln k_s = \ln A_r - \frac{E_r}{R_g T} \quad (4)$$

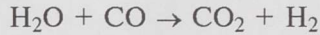
$$\ln D_e = \ln A_d - \frac{E_d}{R_g T} \quad (5)$$

Results and Discussion

Effects of Experimental Conditions on NO_x Emission

Figure 1 gives the effects of several factors on NO_x emission. From these experimental results, some conclusions can be drawn. Generally,

according to the reaction mechanism of NO_x formation, a higher bed temperature enhances the NO_x emission into flue gas. In this study, however, the concentration of NO_x increases below 850°C , and decreases thereafter (see Fig. 1a). This phenomenon can be probably attributed to water shift reaction occurring at the higher temperature, that is



Consequently, a lot of water existing in the reactor promotes reduction of NO_x into N_2 , which decreases NO_x emission at the higher temperature. This conclusion is supported by the fact that the higher moisture content of oil shale reduces the NO_x concentration in flue gas during the oil shale combustion (see Fig 1c). Further research work is necessary to explain the mechanism of NO_x formation.

Figure 1b shows the effects of oil shale particle diameter. The larger particle diameter increases the NO_x concentration in the flue gas. This fact can be explained by catalysis of active components present in shale ash on NO_x formation in oil shale combustion. Further investigation will be needed to discuss the catalytic mechanism of shale ash components on NO_x emission in fluidized bed combustion of oil shale. Figure 1d gives the effect of added limestone on NO_x emission, and also, shale ash addition to the bed has the same effect. From the relationship between Ca/S molar ratio and nitrogen conversion, we can see that the addition of limestone or shale ash for the capture of SO_2 has no influences on NO_x emission.

Kinetic Parameters of NO_x Emission

In this study, Equations (1) to (3) were used to fit experimental data concerning fractional conversion of NO_x emission versus time at different temperatures. The typical results were shown in the Table. The comparison of model predictions with the experimental data was shown in Fig. 2.

Kinetic Parameters of NO_x Emission in Oil Shale Combustion

Parameters	Temperature, $^\circ\text{C}$			
	750	800	850	900
τ , s	120	68	50	37
τ_a , s	28	27	26	23.5
τ_r , s	92	41	24	13.5
τ_r/τ , %	76.7	60.3	48.0	36.5
D_e , cm^2/s	0.2615	0.2850	0.3092	0.3373
K_s , cm/s	2.3886	5.6190	10.048	18.658
F , %	4.3	7.8	8.2	5.7

Relative deviations are reasonably low (<10 %), which implies that the unreacted core model involving ash layer diffusion and chemical reaction can be used to characterize the NO_x emission in fluidized bed combustion of oil shale. The overall burnout time decreases with increasing bed temperature, while τ_a remains approximately unchanged at any temperature. Therefore, temperature has very little effect on ash layer diffusion. The relative importance of ash layer diffusion and chemical reaction varied with temperature. At low temperature (750 °C), the relative proportion of chemical reaction resistance is up to 76.7 %, while at higher temperature (900 °C), it become only 36.5 %. This confirms the fact that chemical reaction is more sensitive to temperature than ash layer diffusion. The reaction rate constant (k_s) and effective ash layer diffusion coefficient (D_e) can be obtained from Equations (4) and (5) using linear regression. These are shown in Equations (6) and (7).

$$k_s = 8.089 \cdot 10^7 \exp\left(-\frac{148457}{R_g T}\right) \text{ cm/s} \quad (6)$$

$$D_e = 2.162 \exp\left(-\frac{18075}{R_g T}\right) \text{ cm}^2/\text{s} \quad (7)$$

From Equations (6) and (7), it is found that the activation energy for chemical reaction is much higher than that for ash layer diffusion (physical process). These results are identical with those from literature [7], which implies that unreacted core model can be reasonably used for modeling of NO_x emission during the fluidized bed combustion of oil shale.

Conclusions

The following conclusions can be drawn from this study:

1. As the bed temperature increases, the concentration of NO_x in flue gas increases below 850 °C, and decreases thereafter. This can be probably attributed to water shaft reaction at higher temperature.
2. The larger oil shale particle diameter increases the NO_x emission during fluidized bed combustion of oil shale.
3. The concentration of NO_x in flue gas decreases with increasing the moisture content of oil shale.
4. Addition of limestone or shale ash to the fluidized bed for SO₂ capture has no effects on NO_x emission during oil shale combustion.
5. A mathematical model with simple expression to describe characteristics of NO_x emission has been developed. The model predictions agree reasonably well with experimental data.
6. The unreacted core model can approximate the combustion of oil shale particles. Both ash layer diffusion and chemical reaction influence the overall burning rate of the particles in the fluidized bed.

Nomenclature

- A_r - frequency factor for chemical reaction, cm/s
 A_d - pre-exponential constant for ash layer diffusion, cm²/s
 C_{Ag} - O₂ concentration in fluidized bed, mol/cm³
 D_e - effective diffusivity of gas in ash layer, cm²/s
 E_r - activation energy for chemical reaction, J/mol
 E_d - apparent activation energy for ash layer diffusion, J/mol
 k_s - intrinsic kinetic constant, cm/s
 R - radius of oil shale particle, cm
 R - gas constant, 8.314 J/molK
 t - time, s
 T - temperature, °C or K
 x - normalized fractional conversion of nitrogen into NO_x
 ρ - density of reactant in oil shale, mol/cm³
 τ - overall burnout time ($\tau = \tau_r + \tau_a$), s
 τ_a - ash layer diffusional contribution to overall burnout time
 τ_r - chemical kinetic contribution to overall burnout time

REFERENCES

1. Miller J. Environment Progress. 1986. No. 5. P. 171.
2. Neathery J. K. Proceedings of International Conference on Fluidized Bed Combustion, ASME, Montreal, Canada, 1991. P. 1511.
3. Henttonen J. Journal of the Institute of Energy. 1992. Vol. 65. P. 118.
4. Wang G. J. et al. Proceedings of 3rd International Conference on Coal Combustion, Beijing, 1995. P. 53.
5. Charlton B. G. Fuel. 1987. Vol. 66. P. 384-387.
6. Li S. Y. et al. Fuel. 1991. Vol. 70. P. 1369.
7. Levenspiel O. "Chemical Reaction Engineering", John Wiley and Sons Inc., New York, 1972.

Received June 25, 1998

VISCOSITY OF SHALE OIL ORIGINATED DISTILLATE OIL - RESIDUAL PETROLEUM OIL BINARY BLENDS

L. MÖLDER
H. TAMVELIUS
L. TIIKMA

Tallinn Technical University,
Institute of Chemistry
15 Akadeemia Rd., Tallinn
12618 Estonia

The evaluation of the kinematic viscosity of shale oil originated distillate oil - residual petroleum oil binary blends is discussed. It is shown that the kinematic viscosity of shale oil originated light "diesel oil" fraction and petroleum originated heavy fuel oil blends can be evaluated by the standard blending calculation technique. When the shale oil originated component is the light gas oil fraction, heavy gas oil fraction or commercial fuel oil, the experimental values of blend kinematic viscosity are always lower than the calculated ones. For such blends, a simple equation can be used for evaluation the difference between the experimental and calculated values of viscosity, depending on the component oil proportion and on the experimental values of viscosity.

In our previous paper [1], it was shown that the kinematic viscosity of shale distillate oil binary blends can be evaluated using the standard blending calculation technique, accepted for hydrocarbon oil blends. This conclusion holds true in spite of the fact that shale oil distillate fractions are mainly made up of the H-bond forming oxygen compounds which often exhibit non-Newtonian properties.

There is only one exception: when the low viscosity component is the shale oil originated light "diesel oil" fraction, the experimental values of blend kinematic viscosity are always higher than the calculated ones. In this event, the difference (Δ) between the logarithms of experimental (v_{exp}) and calculated (v_{calc}) values of blend kinematic viscosity depends on the volume fraction (φ) of component oils (H and L) as well as on v_{exp} . This dependence may be expressed by a simple equation

$$\Delta = P \varphi_H \varphi_L + Q \varphi_H \varphi_L \log v_{\text{exp}} \quad (1)$$

or

$$\frac{\Delta}{\varphi_H \varphi_L} = P + Q \log v_{\text{exp}} \quad (2)$$

where P and Q are constants which depend on the chemical nature of the component oils, but do not depend on component oil proportion.

In this paper, the evaluation of the kinematic viscosity of distillate shale oil - residual petroleum oil binary blends is discussed.

Experimental and Results

Component oils. Oil blends were prepared by blending of commercial shale oil fractions with a long residue from crude petroleum distillation (conventional heavy fuel oil 40).

Shale oil distillate fractions for blending were sampled at *Viru Keemia Grupp AS* (formerly *Kiviter AS*) shale oil distillation unit. Ordinarily, this unit produces distillate fractions as follows:

- Light "diesel oil" fraction: boiling range 180-230 °C, viscosity at 40 °C varies from 1.2 to 1.5 mm²/s
- Light gas oil fraction: boiling range 230-320 °C, viscosity at 50 °C varies from 6 to 15 mm²/s
- Heavy gas oil fraction: boiling range 320-360 °C, viscosity at 50 °C varies from 150 to 250 mm²/s.

By blending these fractions, commercial shale oil originated fuel oils (viscosity at 50 °C from 40 to 80 mm²/s) are produced.

Viscosity characterization constants, A and B (Equation (1) in [2]), of component oil samples which were used for blending are presented in Table 1.

Table 1. Viscosity Characterization Constants of Oil Samples Used for Blending

Component oil	A	B
Shale oil distillates:		
Light "diesel oil" fraction:		
Sample 1	10.30732	4.34029
Sample 2	10.22575	4.31412
Light gas oil fraction:		
Sample 1	12.61017	5.01793
Sample 2	12.34257	4.90101
Heavy gas oil fraction:		
Sample 1	12.25911	4.73897
Sample 2	12.53214	4.85077
Commercial fuel oil	11.41170	4.46849
Petroleum originated heavy fuel oil 40	9.82999	3.78298

Methods. In this work, the kinematic viscosity of distillate shale oil - residual petroleum oil blends, depending on temperature and component oil proportion was studied.

Kinematic viscosity for the component oils and their binary blends with petroleum originated heavy fuel oil was determined in glass capillary viscometers as established by generally accepted standard specifications

[3, 4]. For each blend, viscosity was determined, as a minimum, at 6–8 various temperatures.

For calculation of a blend's "theoretical" viscosity, the Wright standard method [5, 6] was used. Viscosities found using the computer technique [2], similar to that described by Huggins [7], are further interpreted as "calculated" values (ν_{calc}), contrary to the experimental ones (ν_{exp}) measured in the laboratory.

Results. From the results obtained, it follows that the kinematic viscosity of light "diesel oil" fraction binary blends with petroleum originated heavy fuel oil can be evaluated by the standard blending calculation technique accepted for hydrocarbon oil blends. It must be admitted that at smaller φ_H values the values of ν_{exp} are systematically somewhat higher than ν_{calc} (Fig. 1). Nevertheless, these differences are not so essential that the standard calculation technique need to be abandoned.

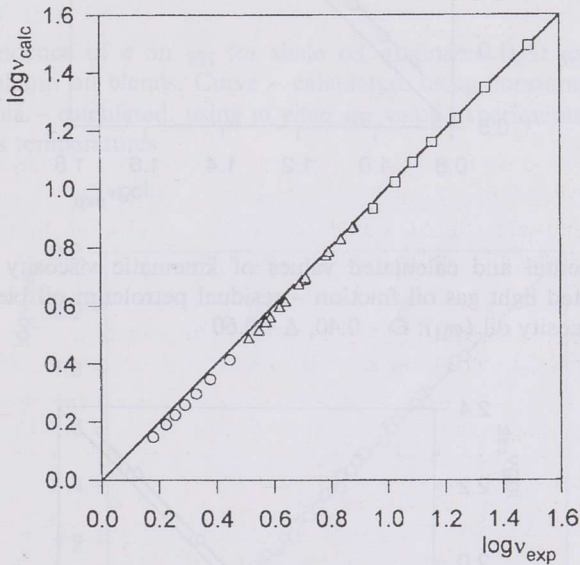


Fig. 1. Experimental (ν_{exp}) and calculated (ν_{calc}) values of kinematic viscosity (mm^2/s) for shale oil originated light "diesel oil" fraction - residual petroleum oil blends. Volume fraction high viscosity oil (φ_H): ○ - 0.25, Δ - 0.50, □ - 0.75

When the petroleum originated heavy fuel oil is blended with shale oil originated commercial fuel oil or with gas oil fractions, both light and heavy, the values of experimental viscosity essentially and systematically differ from calculated ones. As a rule, for these blends, values of ν_{exp} are always lower than ν_{calc} (Figures 2 and 3). In these events, the difference Δ between the logarithms of ν_{exp} and ν_{calc} depends on ν_{exp} . For blends having the constant value of φ_H (or $\varphi_H \varphi_L$), this dependence may be expressed by the following equation

$$\Delta = p + q \log v_{\text{exp}}, \quad (3)$$

where p and q are empirical coefficients, the values of which depend on the volume fraction of component oils.

For each component oil proportion, constants p and q were calculated, using experimental values of viscosity which were measured at 6-8 different temperatures.

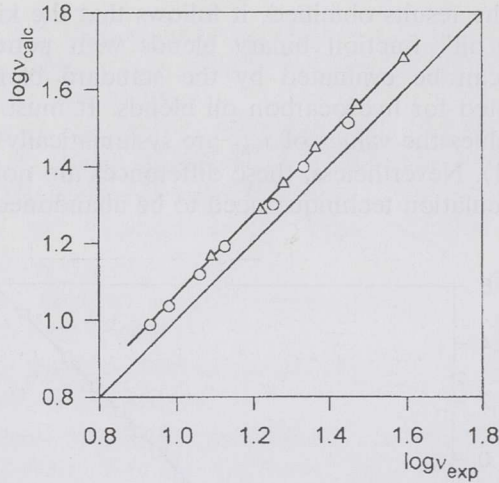


Fig. 2. Experimental and calculated values of kinematic viscosity (mm^2/s) for shale oil originated light gas oil fraction - residual petroleum oil blends. Volume fraction high viscosity oil (ϕ_H): O - 0.40, Δ - 0.60

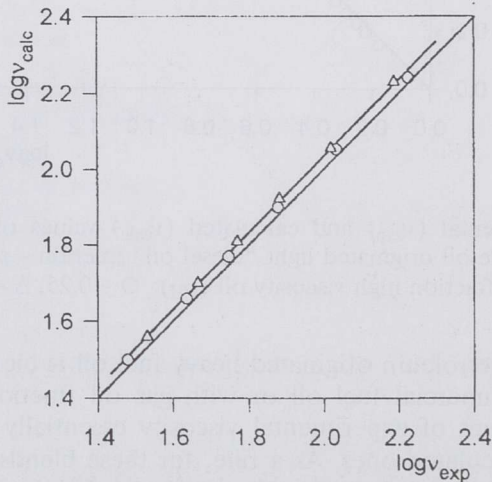


Fig. 3. Experimental and calculated values of kinematic viscosity (mm^2/s) for shale oil originated heavy gas oil fraction - residual petroleum oil blends. Volume fraction high viscosity oil (ϕ_H): O - 0.25, Δ - 0.75

Results obtained (Fig. 4) certify that the dependence of p and q on the volume fraction of components actually can be described as follows from Equations (1) and (2):

$$p = P\varphi_H \varphi_L \tag{4}$$

$$q = Q\varphi_H \varphi_L. \tag{5}$$

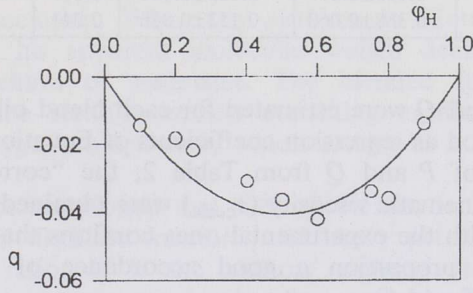


Fig. 4. Dependence of q on φ_H for shale oil originated light gas oil fraction - residual petroleum oil blends. Curve - calculated, using constants P and Q from Table 2. Points - calculated, using at each φ_H value experimental values of ν_{exp} at 6-8 various temperatures

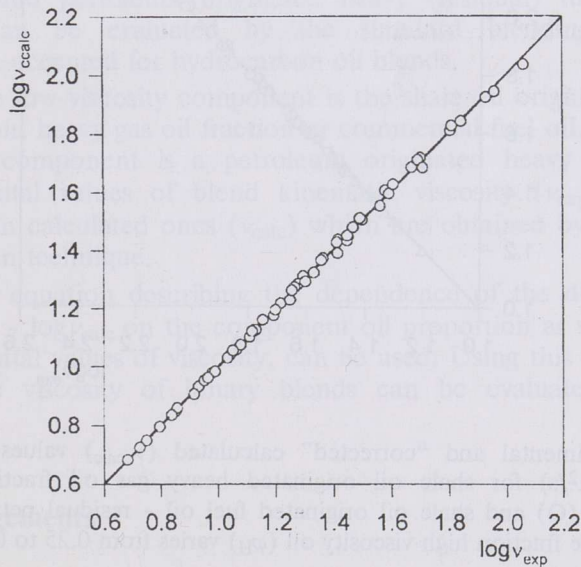


Fig. 5. Experimental and "corrected" calculated (ν_{calc}) values of kinematic viscosity (mm^2/s) for shale oil originated light gas oil fraction - residual petroleum oil blends. Volume fraction high viscosity oil (φ_H) varies from 0.10 to 0.90

Table 2. Constants P and Q for Distillate Shale Oil - Residual Petroleum Oil Binary Blends. Heavy Viscosity Component: Residual Fuel Oil

Low viscosity component	P	Q	s_y^*	Number of experimental values of blend viscosity
Light gas oil fraction	-0.083 ± 0.040	-0.162 ± 0.030	0.076	61
Heavy gas oil fraction	-0.193 ± 0.077	0.032 ± 0.041	0.047	20
Commercial fuel oil	-0.358 ± 0.060	0.153 ± 0.036	0.041	20

$$* y = \Delta / \varphi_H \varphi_L.$$

Constants P and Q were estimated for each blend oil (Table 2) by the least square method as regression coefficients of Equation (2).

Using values of P and Q from Table 2, the "corrected" calculated values of blend kinematic viscosity (v_{ccalc}) were obtained. The comparison of these values with the experimental ones confirms that for all blends at each component proportion a good accordance of results has been reached (Figures 5 and 6).

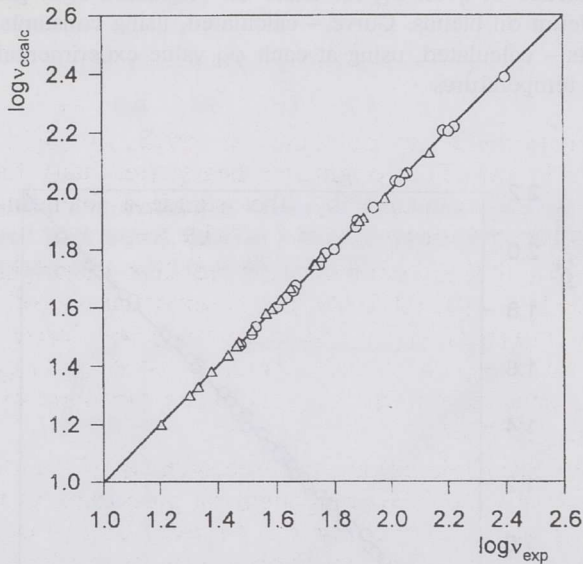


Fig. 6. Experimental and "corrected" calculated (v_{ccalc}) values of kinematic viscosity (mm^2/s) for shale oil originated heavy gas oil fraction - residual petroleum oil (O) and shale oil originated fuel oil - residual petroleum oil (Δ) blends. Volume fraction high viscosity oil (φ_H) varies from 0.25 to 0.75

Results of this study lead to a significant conclusion of applied relevancy: Estonian shale oil distillates may be more effective diluents for heavy petroleum residues than petroleum originated distillates with the same nominal viscosity.

This phenomenon can be explained as a result of the different group composition of shale oil distillates and petroleum originated oils. Shale oil

originated distillate oils are mainly made up of oxygen compounds, especially of resorcinol series phenols, ketones and ethers. Due to the specific composition, associates (H-bond complexes) form between phenolic compounds as proton donors and ketones/ethers as proton acceptors.

Therefore shale oil distillates must be described as a concentrated solution of associates ("polymers"), which exhibits viscosity according to its degree of association. When the distillate is diluted with nonpolar hydrocarbon oil, its apparent molecular weight decreases due to the partial decomposition of associates. The blended fraction makes its contribution to the blend's viscosity according to the lower degree of association of oxygen compounds, which results in a lower viscosity of blend.

It must also be mentioned that fuel oil blends that are produced by blending shale oil distillate fractions and heavy petroleum residues are stable at every ratio. It is the authors' opinion that the approach described in this paper must inspire for more detailed investigations dealing with viscosity and stability of shale oil - petroleum oil blends.

Conclusions

1. The kinematic viscosity of shale oil originated light "diesel oil" fraction and petroleum originated heavy (residual) fuel oil binary blends can be evaluated by the standard blending calculation technique accepted for hydrocarbon oil blends.
2. When the low viscosity component is the shale oil originated light gas oil fraction, heavy gas oil fraction or commercial fuel oil, and the high viscosity component is a petroleum originated heavy fuel oil, the experimental values of blend kinematic viscosity (ν_{exp}) are always lower than calculated ones (ν_{calc}) which are obtained by the standard calculation technique.
3. A simple equation describing the dependence of the difference $\Delta = \log \nu_{\text{exp}} - \log \nu_{\text{calc}}$ on the component oil proportion as well as on the experimental values of viscosity, can be used. Using this approach, the kinematic viscosity of binary blends can be evaluated with great accuracy.

Acknowledgements

This work was financially supported by the Estonian Innovation Foundation, Grant No 46it/98.

REFERENCES

1. Mölder, L., Tamvelius, H., Tiikma, L., Tshuryumova, T. Viscosity of shale oil binary blends // Oil Shale. 1999. V. 16, No. 1. P. 42-50.
2. Mölder, L., Tamvelius, H., Tiikma, L., Tshuryumova, T. Viscosity, stability and compatibility of shale oil distillates // Oil Shale. 1998. V. 15, No. 4. P. 391-397.
3. ASTM D 445. Standard test method for kinematic viscosity of transparent and opaque liquids (and the calculation of dynamic viscosity). 1997 Annual Book of ASTM Standards. V.05.01. Petroleum products and lubricants (I).
4. ISO 3104. Petroleum products. Transparent and opaque liquids. Determination of kinematic viscosity and calculation of dynamic viscosity.
5. Wright, W. A. An improved viscosity - temperature chart for hydrocarbons // Journal of Materials. 1969. V. 4, No. 1. P. 19-27.
6. Manning, R. E. Computational aid for kinematic viscosity conversion from 100 and 210 °F to 40 and 100 °C // Journal of Testing and Evaluation (JTEVA). 1974. V. 2, No. 6. P. 522-528.
7. Huggins, P. Program evaluates component and blend viscosities // Oil and Gas Journal. 1985. V. 83, No. 43. P. 122-129.

Received February 1, 1999